

Performance Assessment of a Centimeter-Scale Four-Stroke Liquid Hydrocarbon-Fueled Glow- Plug Engine

¹Suresh, ²Durga Prasad, ²T. Nibin and ²S. Muthuraman

¹Udaya School of Engineering, Tamilnadu, India

²Jeppiar College of Engineering, Tamilnadu, India

Abstract: Centimeter-scale liquid hydrocarbon-fueled engines have the potential to satisfy the need for high power density mobile power sources. To date, these engines have been in the hobbyist's realm. As a result, engine performance is generally associated with peak power and they have not been optimized for portable power applications which will require high efficiency and reliability and low sound and pollutant emissions levels. Concentrating first on engine efficiency, there are three primary sources of energy loss in centimeter-scale engines: Leaks (i.e., limits in manufacturing tolerances), heat losses (i.e., increased surface to volume ratio and evaporative cooling requirements) and quenching or incomplete combustion (i.e., residence times are too short to allow complete evaporation and combustion or surfaces are cold, quenching the flame and producing incomplete combustion). This research is a first step in the process of modernizing and optimizing miniature engines for a wide range of personal power applications. It includes a reproducible performance assessment of a commercially available four-stroke liquid-fueled glow-plug engine (5 cm³ displacement). The effects of fuel composition and mixture are studied and a first law energy balance is performed to identify the dominant paths of energy loss. Experimental results indicate engine thermal efficiencies between 0.4 and 5.8% and that peak power can vary substantially from manufacturer's specified maximum values. The dominant mode of inefficiency appears to be incomplete combustion.

Key words: Centimeter scale, performance assessment, engine, four-stroke

INTRODUCTION

With the emergence of new mobile technology, there is a great demand for portable power generation devices. The current standard is batteries. Fuel cells are emerging as an alternative to batteries; however their power density is limited by the surface reaction at the triple-phase boundary. Liquid hydrocarbon fuels show promise for future high power density combustion devices. For powering mobile devices, both power density and energy density of the power source are important parameters.

Design trade offs between energy density and power density often arise, as seen in Fig. 1, thus the system must be optimized for the specific application's power requirement. The figure is a standard Rig one plot of existing power sources. In all cases there are regions in the operating domain where there is a trade off between power density and energy density. Note also that electrochemical power sources are generally limited to below 100 W kg⁻¹ in power density, where combustion engines can achieve 1000 W kg⁻¹.

Figure 2 shows the thermal efficiency and power density of various internal combustion engines ranging in size from power plants to miniature engines. Based on manufacturers' claims, the power densities of model engines show great potential for mobile power generation applications if their efficiencies (which correspond to energy densities) can be increased.

Miniature engines first appeared in the model aviation field in the early 1930s (Gierke, 2001). Model engines went through several development and refinement periods over the past 70 years. The early engines were spark-ignited until 1948, when the early glow-ignition period began. Between 1963 and 1969, advances were made in glow-plug ignition. The earliest miniature engines were two stroke cycle because of the mechanical simplicity of their design. Volume production of four-stroke model engines didn't occur until the mid-1970s. From the 1970s to present, model engines went through a refinement period. This period was marked by improvements in materials and manufacturing techniques and refinement of cylinder scavenging designs.

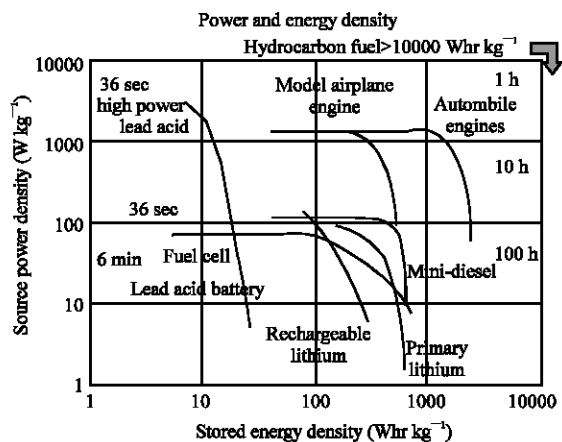


Fig. 1: Power and energy density of power-delivering devices

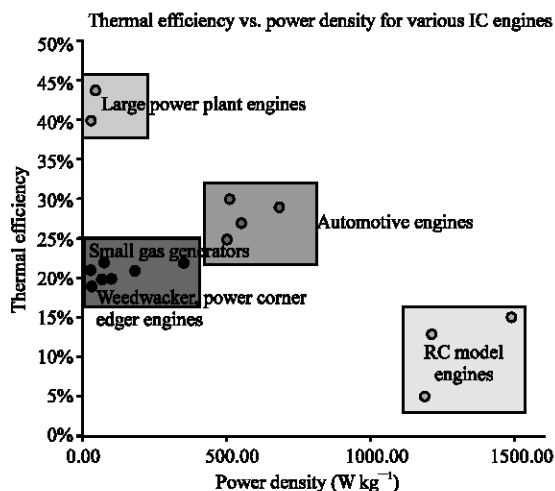


Fig. 2: Efficiency and power density of various IC engines

While miniature engines have been through many years of refinement for use in the model industry (aviation, boating, car-racing) they are not suitably designed for portable power generation applications. There are several features of current production model engines that have become Obstacles to the implementation of this technology for portable power generation: Excessive noise and Vibration, the design of the lubrication and cooling systems, low efficiency and (lack of) combustion control.

DESIGN OF THE O.S. ENGINES FS-30S

The O.S. Engines FS-30S has been chosen for this experiment because it is a good example of a modern, mass-produced model engine design. Fuel delivery is

handled by a carburetor. The air-fuel ratio is varied by manually adjusting a needle valve, thus requiring user intervention. High temperature exhaust gas pressurizes the fuel storage tank. The pressure driving the fuel through the carburetor is influenced by the hydrostatic pressure of the liquid fuel and the temperature of the exhaust products. While this design has the advantage of simplifying the balance of plant, it contaminates the fuel supply with exhaust products and results in inconsistency in the reactant stoichiometry. The engine displacement is 5 cm³. It is a single cylinder, single-ringed piston design. There is one inlet valve and one valve for exhaust. Lubrication of the engine parts is handled by premixing the fuel with oil. This simplifies the engine design, but has inherent flaws. All of the unburned oil is exhausted into the atmosphere and its high vapor pressure means that it deposits on surfaces throughout the immediate surroundings of the engine.

Fuels: Fuels for model engines are composed of methanol (CH₃OH), nitro methane (CH₃NO₂) and oil. Typical mixtures are 10-20% (by volume) oil, 0-50% nitro methane and a balance of methanol. Ideally, the oil component of the fuel does not contribute to the heating value of the fuel. Synthetic based oils, castor-based oils and mixtures of the two are used exclusively for lubrication. Because of their proprietary nature, it is difficult to find any useful information about synthetic-based oils. All of our experimental results have been obtained using castor oil (C₁₈H₃₄O₃) as the sole lubricant. Castor oil is a very good lubricant: the coefficient of friction for castor oil with steel on steel is 0.095 (Weast, 2003). It is thick, clear-yellowish oil extracted from the seeds of the castor bean plant, *ricinus communist*. Its composition is approximately 89% riciniolic acid, with approximately 11% other fatty acids as shown in Fig. 3. As it is heated, it forms complex polymers which continue to provide excellent lubrication properties. Its spontaneous ignition temperature is 449°C. The heat of combustion of castor oil is 39.5 MJ kg⁻¹ (Heywood, 1998). Thus, if burned, it would contribute greatly to the heating value of the fuel mixture.

The spontaneous ignition temperatures of methanol and nitro methane are 574 and 419°C respectively (Mullins, 1955). Glow plug temperatures are typically between 700 and 800°C, therefore while pure methanol fuel will ignite, fuel mixtures with higher concentrations of nitro methane will ignite more readily. The Lower Heating Value (LHV) of methanol is 20.0 MJ kg⁻¹ and the LHV of nitro methane is 11.3 MJ kg⁻¹, thus it is apparent that the energy density (kJ g⁻¹) of a fuel mixture with a high nitro methane concentration will be lower than that of a fuel mixture with a low concentration. While the addition of

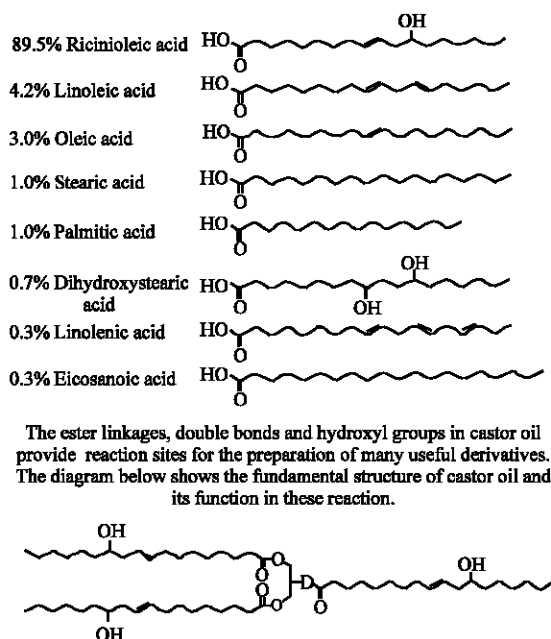


Fig. 3: The composition and chemical structure of castor oil

nitro methane reduces the overall heating value of the fuel mixture, the advantage of adding nitro methane is that the ratio of chemical energy to volume of the combustible stoichiometric reactant mixture increases.

The nitro methane molecule contains two oxygen atoms. The methanol molecule contains only one oxygen atom. Nitro methane acts as an oxygen carrier, requiring less air for combustion than methanol, hence it allows a greater volume of fuel into the same size combustion chamber. The stoichiometric Air/Fuel ratio (A/F) of methanol and nitro methane is 6.47 and 1.70, respectively. Figure 4 is a plot of fuel energy density and energy/volume ratio as a function of nitro methane molar ratio for a fuel mixture of pure nitro methane and methanol.

Efficiency and scaling: Theoretical model engine efficiency, η_{th} , can be described by either the Otto cycle or the Diesel cycle, depending on whether it is spark ignited or compression ignited. For both cases, the theoretical thermal efficiency is independent of engine size. When scaling down to smaller sizes, however, the surface area-to-volume ratio increases, thereby amplifying losses. The dominant loss mechanisms are heat transfer, flame quenching, and leakage past the piston ring (Annen *et al.*, 2003). Leakage reduces the compression ratio and facilitates incomplete combustion. The precision of the tolerance fit between the piston and cylinder is limited by surface finish, alignment and the need to

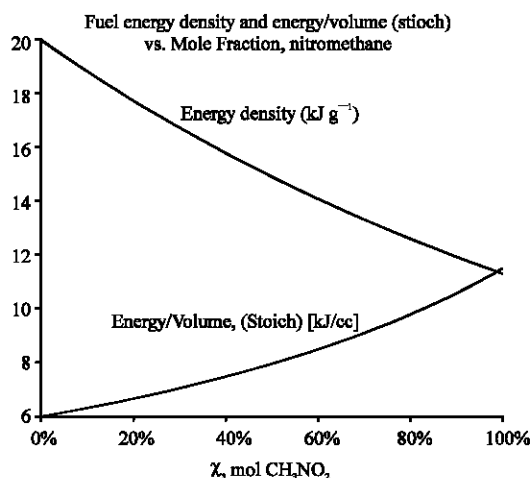


Fig. 4: Energy density and energy/volume ratio vs. nitro methane molar ratio

minimize frictional losses. It is standard practice to describe engine efficiency with the fuel conversion efficiency:

$$\eta_f = \text{Fuel conversion efficiency} = \frac{W_c}{\dot{m} Q_{HV}} \text{ (Heywood, 1988)}$$

$$\text{If the fuel is a mixture, then } \eta_f = \frac{W_{brake}}{\sum_{i=1}^n \dot{m}_i Q_{LHV,i}}$$

A very important concern for model engine fuels is whether or not to include the heating value of the lubricant in the efficiency calculation. Since the castor oil used in this experiment is a possible contributor to the heating value, it will be included in the efficiency calculations that follow.

DESIGN OF THE EXPERIMENT

The O.S. Engines FS-30-S four stroke model engines is the subject of this preliminary study. The angular velocity of the engine shaft is measured optically by measuring the frequency of the reflections of a helium-neon laser. The light is reflected off of the engine shaft once per crankshaft revolution and focused onto a fast photodiode, which outputs a periodic waveform corresponding to the the angular velocity of the engine, ω . A measured load is applied to the engine via a belt and pulley system connected to an Ever Motor ERS-380PM-3270 Permanent Magnet (PM) DC electric motor. Due to the interaction between the stator field and the armature current, the torque generated by a PM DC electric motor is directly proportional to the armature

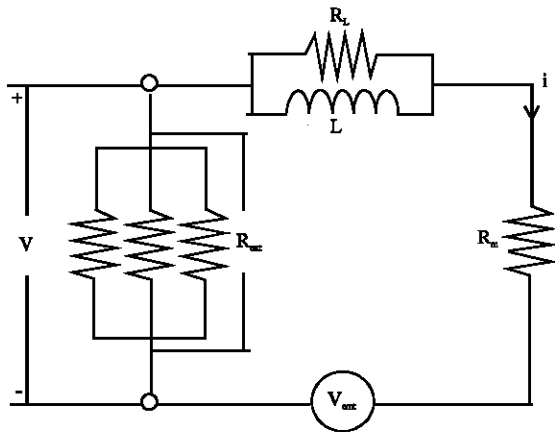


Fig. 5: The electrical circuit of the dynamometer system

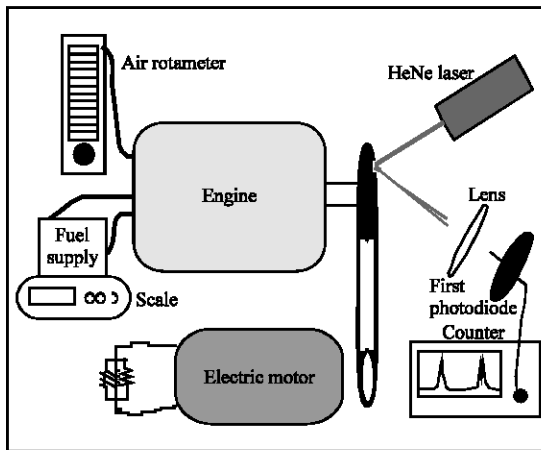


Fig. 6: Block diagram of the experimental setup

current. The value of the torque constant, k_T , is 5.16 mN-m/A. The electric motor is connected in parallel to a series of resistors. The external resistance, R_{ext} , can be varied between 0.6 and 10.0 ohm. An increase in external resistance results in a reduction of the applied load. The voltage, V , between the electric motor's positive and negative terminals is measured. From this voltage measurement the torque, T , of the engine is calculated by:

$$T = \frac{D_2}{D_1} \frac{k_T \cdot V}{R_{ext}}$$

Where D_2 and D_1 are the diameters of the pulleys attached to the engine and the electric motor, respectively.

Figure 5 shows the electrical circuit of the dynamometer system. The mechanical power of the engine is the product of angular velocity and torque $P = T \cdot \omega$.

Fuel mixture	Fuel constiment	Xvol	Max power	Max efficiency
A	Methanol mitromethane castor oil	79% 3% 18%	48.0W	3.5%
B	Methanol mitromethane castor oil	72% 10% 18%	82.9W	5.8%
C	Methanol mitromethane castor oil	62% 20% 18%	48.3W	3.5%

Fig. 7: Max steady state power and efficiency of fuel mixtures

The fuel flow rate measurement is determined by taking a series of measurements of the mass of the fuel in the fuel tank. The fuel mass flow rate is then calculated from a least squares fit of the data.

The intake air volumetric flow rate is measured by a Rota meter. To prevent thermal failure of the engine components, a 77 CFM fan provides external cooling.

Steady state operation is achieved over a two minute warm-up period before data is acquired. A fixed load setting is applied to the engine and a fixed angular velocity is maintained for approximately ten minutes, while measurements are logged. A schematic of the experimental setup is shown in Fig. 6.

RESULTS

The engine was tested with three fuels, each with 18% castor oil lubricant (manufacturer's specified minimum value). The maximum steady-state power achieved was 82.9 W, significantly less than the O.S. Engines' claimed maximum power of 0.5 brake horsepower (373 W). This is shown in Fig. 7. The maximum power and efficiency was obtained with fuel mixture B.

The operating torque seems to have a stronger influence on efficiency than angular velocity does. This is shown in Fig. 8. Higher efficiencies occur as torque and angular velocity are increased. The maximum steady-state torque sustainable for fuel mixtures A, B and C are 51.6, 60.4 and 55.0 mN-m, respectively.

The measured equivalence ratio is less than one for all data points taken in this experiment. Figure 9 shows that the efficiency is greatest at the lowest equivalence ratios sustainable. As shown in Fig. 10, power is also greatest at the lowest equivalence ratios sustainable.

The fuel-lean limit occurs when the flame is quenched by excess air and the engine abruptly stalls. The maximum performance (peak power and efficiency) occurs just before the threshold of excess air-induced stalling.

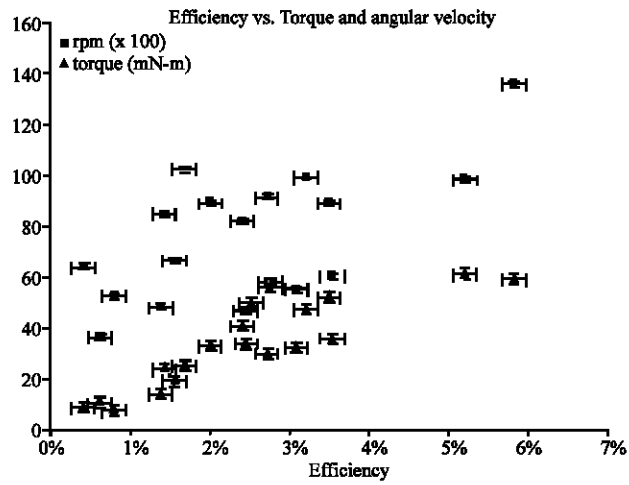


Fig. 8: Efficiency vs. Torque and angular velocity

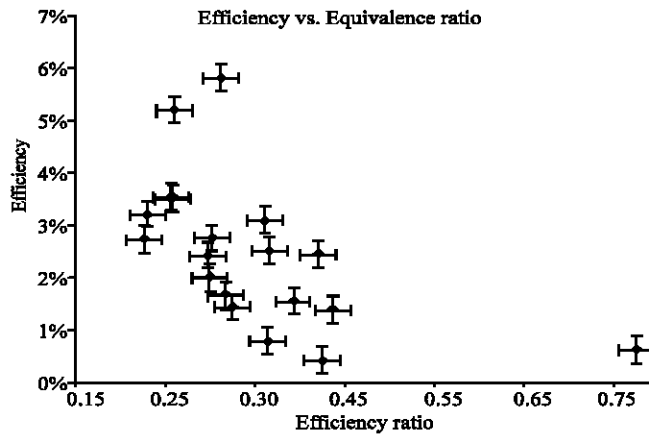


Fig. 9: Efficiency vs. Equivalence ratio

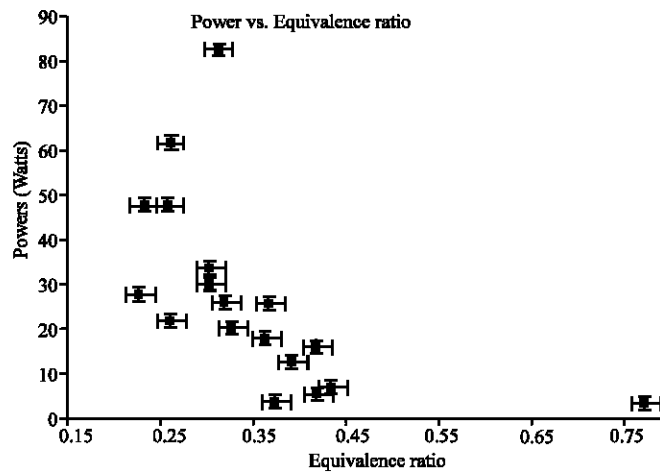


Fig. 10: Power vs. Equivalence ratio

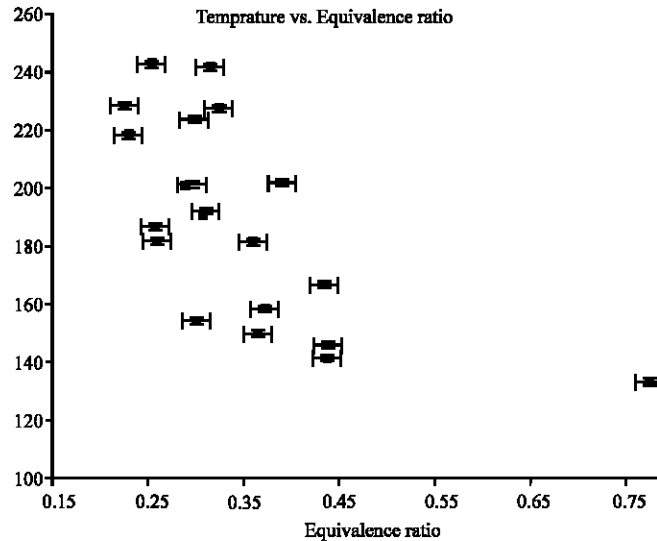


Fig. 11: Engine crankcase Temperature vs. Equivalence ratio

The temperature of the engine crankcase increases as the equivalence ratio is decreased, as seen in Fig. 11. We do not see a peak in engine temperature before the engine stalls due to excess air. We are led to believe that the combustible mixture is not fully mixed in the combustion chamber, thus leading to flame quenching.

CONCLUSION

There is great potential to improve the performance of current production model engines for portable power application. The most important issues that should be addressed are the lubrication system and fuel/air delivery system.

The lubrication system must be modified before these engines can be used for portable power generation applications because the addition of inert oil into the combustion chamber reduces the power density of the system by lowering the reactant concentration/volume ratio and causes excess emissions of unburned hydrocarbon oils. The addition of inert oil into the fuel storage tank also reduces the extractable energy density of the fuel (the overall energy density is higher, but the oil is not fully combusted). If the heating value of the oil is not considered in the efficiency calculation, then the peak efficiency measured jumps from 5.8 to 9.3%.

The design of the fuel/air delivery system should be improved to facilitate mixing of the fuel/air mixture prior to ignition. The carburetor design does not sufficiently atomize the reactants, resulting in incomplete combustion. Furthermore, the needle valve adjustment on the carburetor is very sensitive and requires user intervention. For practical application the reactant delivery process should utilize a feedback controller requiring no end-user input.

The O.S. Engines FS-30-S achieved maximum performance with the fuel mixture containing 62% methanol, 18% castor oil and 10% nitro methane. We expected that engine performance would increase with higher concentrations of nitro methane; however that was not the case. The engine ignition timing depends on the glow plug temperature and the pressure of the reactants (compression ratio). These parameters should be optimized for the specific fuel mixture that the engine is designed to operate on. We intend to study additional engines to determine the engine-engine variability of these findings.

A rough estimate of the convective heat transfer assuming a transitional Reynolds' number (Re), surface temperature of 500 K and surface area of 10 cm² gives 10-20 W of heat transfer losses. While significant in comparison to mechanical power production, it only amounts to a few percent of the total chemical energy of the fuel. Incomplete combustion appears to be the dominant path of energy loss.

REFERENCES

Annen K., D. Stickler and J. Woodroffe, 2003. Linearly-Oscillating Miniature International Combustion Engine (MICE) for Portable Electric Power. American Institute of Aeronautics and Astronautics Conference, Reno, NV.
 Gierke, D., 2001. 2-Stroke Glow Engines for R/C Aircraft, Air Age Inc, Vol. 1.
 Heywood, 1998. J. Int. Combustion Engine Fundamentals, McGraw-Hill Publishing Co.
 Mullins, 1955. AGARDO graph No.4.
 Weast, R., 2003. Handbook of Chemistry and Physics, The Chemical Rubber Co.